

Chapter 3: Electromagnetic Fields in Simple Devices and Circuits

3.1 *Resistors and capacitors*

3.1.1 Introduction

One important application of electromagnetic field analysis is to simple electronic components such as resistors, capacitors, and inductors, all of which exhibit at higher frequencies characteristics of the others. Such structures can be analyzed in terms of their: 1) static behavior, for which we can set $\partial/\partial t = 0$ in Maxwell's equations, 2) quasistatic behavior, for which $\partial/\partial t$ is non-negligible, but we neglect terms of the order $\partial^2/\partial t^2$, and 3) dynamic behavior, for which terms on the order of $\partial^2/\partial t^2$ are not negligible either; in the dynamic case the wavelengths of interest are no longer large compared to the device dimensions. Because most such devices have either cylindrical or planar geometries, as discussed in Sections 1.3 and 1.4, their fields and behavior are generally easily understood. This understanding can be extrapolated to more complex structures.

One approach to analyzing simple structures is to review the basic constraints imposed by symmetry, Maxwell's equations, and boundary conditions, and then to hypothesize the electric and magnetic fields that would result. These hypotheses can then be tested for consistency with any remaining constraints not already invoked. To illustrate this approach resistors, capacitors, and inductors with simple shapes are analyzed in Sections 3.1–2 below.

All physical elements exhibit varying degrees of resistance, inductance, and capacitance, depending on frequency. This is because: 1) essentially all conducting materials exhibit some resistance, 2) all currents generate magnetic fields and therefore contribute inductance, and 3) all voltage differences generate electric fields and therefore contribute capacitance. R's, L's, and C's are designed to exhibit only one dominant property at low frequencies. Section 3.3 discusses simple examples of ambivalent device behavior as frequency changes.

Most passive electronic components have two or more terminals where voltages can be measured. The voltage difference between any two terminals of a passive device generally depends on the histories of the currents through all the terminals. Common passive linear two-terminal devices include resistors, inductors, and capacitors (R's, L's, and C's, respectively), while transformers are commonly three- or four-terminal devices. Devices with even more terminals are often simply characterized as N-port networks. Connected sets of such passive linear devices form passive linear circuits which can be analyzed using the methods discussed in Section 3.4. RLC resonators and RL and RC relaxation circuits are most relevant here because their physics and behavior resemble those of common electromagnetic systems. RLC resonators are treated in Section 3.5, and RL, RC, and LC circuits are limiting cases when one of the three elements becomes negligible.

3.1.2 Resistors

Resistors are two-terminal passive linear devices characterized by their *resistance* R [ohms]:

$$v = iR \quad (3.1.1)$$

where $v(t)$ and $i(t)$ are the associated voltage and current. That is, one volt across a one-ohm resistor induces a one-ampere current through it; this defines the *ohm*.

The resistor illustrated in Figure 3.1.1 is comprised of two parallel perfectly conducting end-plates between which is placed a medium of conductivity σ , permittivity ϵ , permeability μ , and thickness d ; the two end plates and the medium all have a constant cross-sectional area A [m²] in the x - y plane. Let's assume a static voltage v exists across the resistor R , and that a current i flows through it.

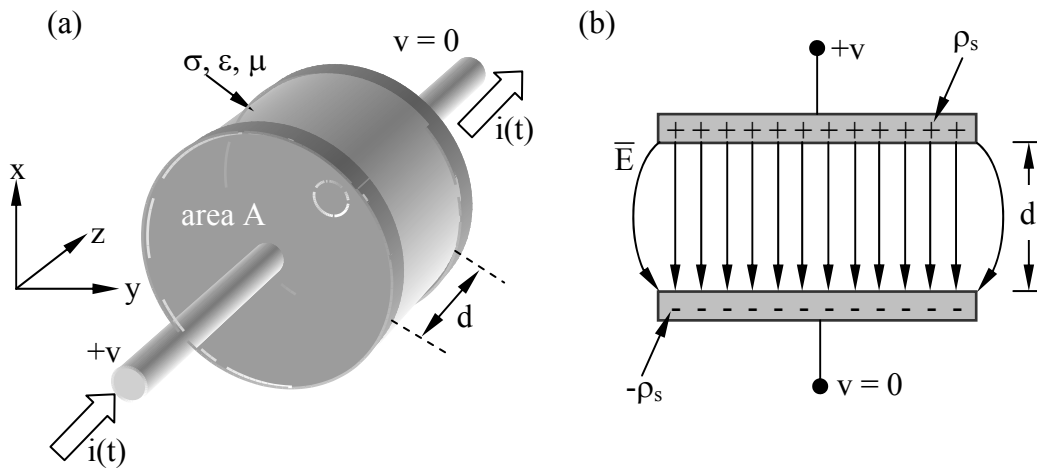


Figure 3.1.1 Simple resistor.

Boundary conditions require the electric field \bar{E} at any perfectly conducting plate to be perpendicular to it [see (2.6.16); $\bar{E} \times \hat{n} = 0$], and Faraday's law requires that any line integral of \bar{E} from one iso-potential end plate to the other must equal the voltage v regardless of the path of integration (1.3.13). Because the conductivity σ [Siemens/m] is uniform within walls parallel to \hat{z} , these constraints are satisfied by a static uniform electric field $\bar{E} = \hat{z}E_0$ everywhere within the conducting medium, which would be charge-free since our assumed \bar{E} is non-divergent. Thus:

$$\int_0^d \bar{E} \cdot \hat{z} dz = E_0 d = v \quad (3.1.2)$$

where $E_0 = v/d$ [Vm⁻¹].

Such an electric field within the conducting medium induces a current density \bar{J} , where:

$$\bar{J} = \sigma \bar{E} \text{ [Am}^{-2}\text{]} \quad (3.1.3)$$

The total current i flowing is the integral of $\bar{\mathbf{J}} \cdot \hat{\mathbf{z}}$ over the device cross-section A , so that:

$$i = \iint_A \bar{\mathbf{J}} \cdot \hat{\mathbf{z}} \, dx dy = \iint_A \sigma \bar{\mathbf{E}} \cdot \hat{\mathbf{z}} \, dx dy = \iint_A \sigma E_0 \, dx dy = \sigma E_0 A = v \sigma A / d \quad (3.1.4)$$

But $i = v/R$ from (3.1.1), and therefore the static resistance of a simple *planar resistor* is:

$$R = v/i = d/\sigma A \text{ [ohms]} \quad (3.1.5)$$

The instantaneous power p [W] dissipated in a resistor is $i^2 R = v^2/R$, and the time-average power dissipated in the sinusoidal steady state is $|I|^2 R/2 = |V|^2/2R$ watts. Alternatively the local instantaneous power density $P_d = \bar{\mathbf{E}} \cdot \bar{\mathbf{J}}$ [W m⁻³] can be integrated over the volume of the resistor to yield the total instantaneous power dissipated:

$$p = \iiint_V \bar{\mathbf{E}} \cdot \bar{\mathbf{J}} \, dv = \iiint_V \bar{\mathbf{E}} \cdot \sigma \bar{\mathbf{E}} \, dv = \sigma |\bar{\mathbf{E}}|^2 A d = \sigma A v^2 / d = v^2/R \text{ [W]} \quad (3.1.6)$$

which is the expected answer, and where we used (2.1.17): $\bar{\mathbf{J}} = \sigma \bar{\mathbf{E}}$.

Surface charges reside on the end plates where the electric field is perpendicular to the perfect conductor. The boundary condition $\hat{\mathbf{n}} \cdot \bar{\mathbf{D}} = \rho_s$ (2.6.15) suggests that the surface charge density ρ_s on the positive end-plate face adjacent to the conducting medium is:

$$\rho_s = \epsilon E_0 \text{ [Cm}^{-2}\text{]} \quad (3.1.7)$$

The total static charge Q on the positive resistor end plate is therefore $\rho_s A$ coulombs. By convention, the subscript s distinguishes surface charge density ρ_s [C m⁻²] from volume charge density ρ [C m⁻³]. An equal negative surface charge resides on the other end-plate. The total stored charged $Q = \rho_s A = CV$, where C is the device capacitance, as discussed further in Section 3.1.3.

The static currents and voltages in this resistor will produce fields outside the resistor, but these produce no additional current or voltage at the device terminals and are not of immediate concern here. Similarly, μ and ϵ do not affect the static value of R . At higher frequencies, however, this resistance R varies and both inductance and capacitance appear, as shown in the following three sections. Although this static solution for charge, current, and electric field within the conducting portion of the resistor satisfies Maxwell's equations, a complete solution would also prove uniqueness and consistency with $\bar{\mathbf{H}}$ and Maxwell's equations outside the device. Uniqueness is addressed by the uniqueness theorem in Section 2.8, and approaches to finding fields for arbitrary device geometries are discussed briefly in Sections 4.4–6.

Example 3.1A

Design a practical 100-ohm resistor. If thermal dissipation were a problem, how might that change the design?

Solution: Resistance $R = d/\sigma A$ (3.1.5), and if we arbitrarily choose a classic cylindrical shape with resistor length $d = 4r$, where r is the radius, then $A = \pi r^2 = \pi d^2/16$ and $R = 16/\pi d\sigma = 100$. Discrete resistors are smaller for modern low power compact circuits, so we might set $d = 1$ mm, yielding $\sigma = 16/\pi dR = 16/(\pi 10^{-3} \times 100) \cong 51 \text{ S m}^{-1}$. Such conductivities roughly correspond, for example, to very salty water or carbon powder. The surface area of the resistor must be sufficient to dissipate the maximum power expected, however. Flat resistors thermally bonded to a heat sink can be smaller than air-cooled devices, and these are often made of thin metallic film. Some resistors are long wires wound in coils. Resistor failure often occurs where the local resistance is slightly higher, and the resulting heat typically increases the local resistance further, causing even more local heating.

3.1.3 Capacitors

Capacitors are two-terminal passive linear devices storing charge Q and characterized by their *capacitance* C [Farads], defined by:

$$Q = Cv \text{ [Coulombs]} \quad (3.1.8)$$

where $v(t)$ is the voltage across the capacitor. That is, one static volt across a one-Farad capacitor stores one Coulomb on each terminal, as discussed further below; this defines the *Farad* [Coulombs per volt].

The resistive structure illustrated in Figure 3.1.1 becomes a pure capacitor at low frequencies if the media conductivity $\sigma \rightarrow 0$. Although some capacitors are air-filled with $\epsilon \cong \epsilon_0$, usually dielectric filler with permittivity $\epsilon > \epsilon_0$ is used. Typical values for the *dielectric constant* ϵ/ϵ_0 used in capacitors are ~ 1 -100. In all cases boundary conditions again require that the electric field \bar{E} be perpendicular to the perfectly conducting end plates, i.e., to be in the $\pm z$ direction, and Faraday's law requires that any line integral of \bar{E} from one iso-potential end plate to the other must equal the voltage v across the capacitor. These constraints are again satisfied by a static uniform electric field $\bar{E} = zE_0$ within the medium separating the plates, which is uniform and charge-free.

We shall neglect temporarily the effects of all fields produced outside the capacitor if its plate separation d is small compared to its diameter, a common configuration. Thus $E_0 = v/d$ [V m⁻¹] (3.1.2). The surface charge density on the positive end-plate face adjacent to the conducting medium is $\sigma_s = \epsilon E_0$ [C m⁻²], and the total static charge Q on the positive end plate of area A is therefore:

$$Q = A\sigma_s = A\epsilon E_0 = A\epsilon v/d = Cv \text{ [C]} \quad (3.1.9)$$

Therefore, for a *parallel-plate capacitor*:

$$C = \epsilon A/d \text{ [Farads]} \quad (\text{parallel-plate capacitor}) \quad (3.1.10)$$

Using (3.1.2) and the fact that the charge $Q(t)$ on the positive plate is the time integral of the current $i(t)$ into it, we obtain the relation between voltage and current for a capacitor:

$$v(t) = Q(t)/C = (1/C) \int_{-\infty}^t i(t) dt \quad (3.1.11)$$

$$i(t) = C \, dv(t)/dt \quad (3.1.12)$$

When two capacitors are connected in parallel as shown in Figure 3.1.2, they are equivalent to a single capacitor of value C_{eq} storing charge Q_{eq} , where these values are easily found in terms of the charges (Q_1, Q_2) and capacitances (C_1, C_2) associated with the two separate devices.

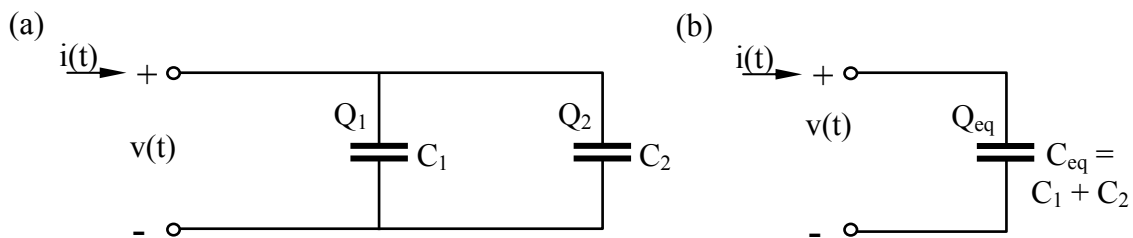


Figure 3.1.2 Capacitors in parallel.

Because the total charge Q_{eq} is the sum of the charges on the two separate capacitors, and capacitors in parallel have the same voltage v , it follows that:

$$Q_{eq} = Q_1 + Q_2 = (C_1 + C_2)v = C_{eq}v \quad (3.1.13)$$

$$C_{eq} = C_1 + C_2 \quad (\text{capacitors in parallel}) \quad (3.1.14)$$

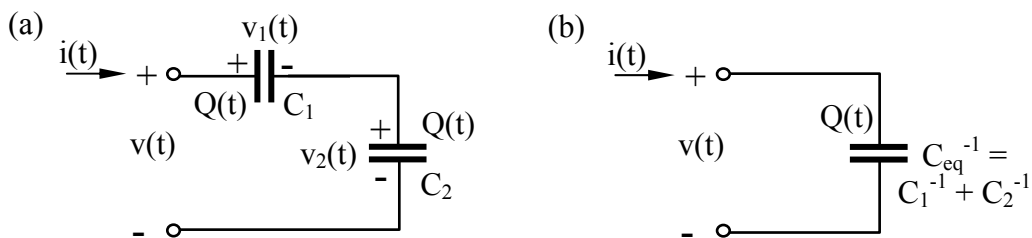


Figure 3.1.3 Capacitors in series.

When two capacitors are connected in series, as illustrated in Figure 3.1.3, then their two charges Q_1 and Q_2 remain equal if they were equal before current $i(t)$ began to flow, and the total voltage is the sum of the voltages across each capacitor:

$$C_{eq}^{-1} = v/Q = (v_1 + v_2)/Q = C_1^{-1} + C_2^{-1} \quad (\text{capacitors in series}) \quad (3.1.15)$$

The instantaneous electric energy density W_e [$J\ m^{-3}$] between the capacitor plates is given by Poynting's theorem: $W_e = \epsilon |\bar{E}|^2 / 2$ (2.7.7). The total electric energy w_e stored in the capacitor is the integral of W_e over the volume Ad of the dielectric:

$$w_e = \iiint_V \left(\epsilon |\bar{E}|^2 / 2 \right) dv = \epsilon Ad |\bar{E}|^2 / 2 = \epsilon Av^2 / 2d = Cv^2 / 2 \quad [J] \quad (3.1.16)$$

The corresponding expression for the time-average energy stored in a capacitor in the sinusoidal steady state is:

$$w_e = C |\underline{V}|^2 / 4 \quad [] \quad (3.1.17)$$

The extra factor of two relative to (3.1.9) enters because the time average of a sinusoid squared is half its peak value.

To prove (3.1.16) for any capacitor C , not just parallel-plate devices, we can compute $w_e = \int_0^t i v dt$ where $i = dq/dt$ and $q = Cv$. Therefore $w_e = \int_0^t C (dv/dt) v dt = \int_0^v Cv dv = Cv^2/2$ in general.

We can also analyze other capacitor geometries, such as the cylindrical capacitor illustrated in Figure 3.1.4. The inner radius is "a", the outer radius is "b", and the length is D ; its interior has permittivity ϵ .

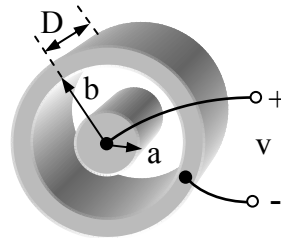


Figure 3.1.4 Cylindrical capacitor.

The electric field again must be divergence- and curl-free in the charge-free regions between the two cylinders, and must be perpendicular to the inner and outer cylinders at their perfectly conducting walls. The solution can be cylindrically symmetric and independent of ϕ . A purely radial electric field has these properties:

$$\bar{E}(r) = rE_o/r \quad (3.1.18)$$

The electric potential $\Phi(r)$ is the integral of the electric field, so the potential difference v between the inner and outer conductors is:

$$v = \Phi_a - \Phi_b = \int_a^b \frac{E_o}{r} dr = E_o \ln r \Big|_a^b = E_o \ln\left(\frac{b}{a}\right) \text{ [V]} \quad (3.1.19)$$

This capacitor voltage produces a surface charge density ρ_s on the inner and outer conductors, where $\rho_s = \epsilon E = \epsilon E_o/r$. If $\Phi_a > \Phi_b$, then the inner cylinder is positively charged, the outer cylinder is negatively charged, and E_o is positive. The total charge Q on the inner cylinder is then:

$$Q = \rho_s 2\pi a D = \epsilon E_o 2\pi D = \epsilon v 2\pi D / \left[\ln(b/a) \right] = C v \text{ [C]} \quad (3.1.20)$$

Therefore this *cylindrical capacitor* has capacitance C :

$$C = \epsilon 2\pi D / \left[\ln(b/a) \right] \text{ [F]} \quad (\text{cylindrical capacitor}) \quad (3.1.21)$$

In the limit where $b/a \rightarrow 1$ and $b - a = d$, then we have approximately a parallel-plate capacitor with $C \rightarrow \epsilon A/d$ where the plate area $A = 2\pi a D$; see (3.1.10).

Example 3.1B

Design a practical 100-volt 10^{-8} farad (0.01 mfd) capacitor using dielectric having $\epsilon = 20\epsilon_o$ and a breakdown field strength E_B of 10^7 [V m⁻¹].

Solution: For parallel-plate capacitors $C = \epsilon A/d$ (3.1.10), and the device breakdown voltage is $E_B d = 100$ [V]. Therefore the plate separation $d = 100/E_B = 10^{-5}$ [m]. With a safety factor of two, d doubles to 2×10^{-5} , so $A = dC/\epsilon = 2 \times 10^{-5} \times 10^{-8} / (20 \times 6.85 \times 10^{-12}) \cong 1.5 \times 10^3$ [m²]. If the capacitor is a cube of side D , then the capacitor volume is $D^3 = Ad$ and $D = (Ad)^{0.333} = (1.5 \times 10^{-3} \times 2 \times 10^{-5})^{0.333} \cong 3.1$ mm. To simplify manufacture, such capacitors are usually wound in cylinders or cut from flat stacked sheets.

3.2 Inductors and transformers

3.2.1 Solenoidal inductors

All currents in devices produce magnetic fields that store magnetic energy and therefore contribute inductance to a degree that depends on frequency. When two circuit branches share magnetic fields, each will typically induce a voltage in the other, thus *coupling* the branches so they form a transformer, as discussed in Section 3.2.4.

Inductors are two-terminal passive devices specifically designed to store magnetic energy, particularly at frequencies below some design-dependent upper limit. One simple geometry is shown in Figure 3.2.1 in which current $i(t)$ flows in a loop through two perfectly conducting parallel plates of width W and length D , spaced d apart, and short-circuited at one end.

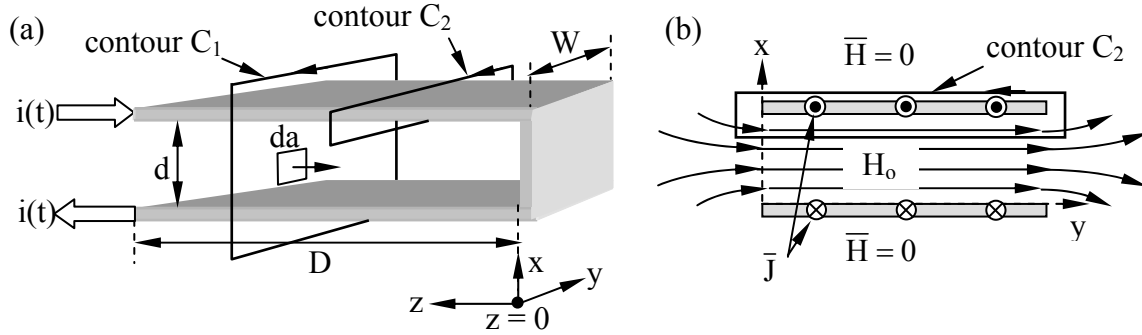


Figure 3.2.1 Parallel-plate inductor.

To find the magnetic field from the currents we can use the integral form of Ampere's law, which links the variables \bar{H} and \bar{J} :

$$\oint_C \bar{H} \cdot d\bar{s} = \iint_A (\bar{J} + \partial\bar{D}/\partial t) \cdot d\bar{a} \quad (3.2.1)$$

The contour C_1 around both currents in Figure 3.2.1 encircles zero net current, and (3.2.1) says the contour integral of \bar{H} around zero net current must be zero in the static case. Contour C_2 encircles only the current $i(t)$, so the contour integral of \bar{H} around any C_2 in the right-hand sense equals $i(t)$ for the static case. The values of these two contour integrals are consistent with zero magnetic field outside the pair of plates and a constant field $\bar{H} = H_0 \hat{y}$ between them, although a uniform magnetic field could be superimposed everywhere without altering those integrals. Since such a uniform field would not have the same symmetry as this device, such a field would have to be generated elsewhere. These integrals are also exactly consistent with fringing fields at the edges of the plate, as illustrated in Figure 3.2.1(b) in the x - y plane for $z > 0$. Fringing fields can usually be neglected if the plate separation d is much less than the plate width W .

It follows that:

$$\oint_{C_2} \bar{H} \cdot d\bar{s} = i(t) = H_0 W \quad (3.2.2)$$

$$\bar{H} = \hat{y} H_0 = \hat{y} i(t)/W \quad [\text{A m}^{-1}] \quad (\bar{H} \text{ between the plates}) \quad (3.2.3)$$

and $\bar{H} \cong 0$ elsewhere.

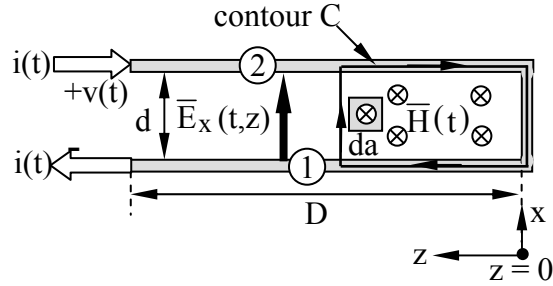


Figure 3.2.2 Voltages induced on a parallel-plate inductor.

The voltage $v(t)$ across the terminals of the inductor illustrated in Figures 3.2.1 and 3.2.2 can be found using the integral form of Faraday's law and (3.2.3):

$$\oint_C \bar{E} \cdot d\bar{s} = -\frac{\partial}{\partial t} \iint_A \mu \bar{H} \cdot d\bar{a} = -\frac{\mu D d}{W} \frac{di(t)}{dt} = \int_1^2 E_x(t,z) dx = -v(t,z) \quad (3.2.4)$$

where $z = D$ at the inductor terminals. Note that when we integrate \bar{E} around contour C there is zero contribution along the path inside the perfect conductor; the non-zero portion is restricted to the illustrated path 1-2. Therefore:

$$v(t) = \frac{\mu D d}{W} \frac{di(t)}{dt} = L \frac{di(t)}{dt} \quad (3.2.5)$$

where (3.2.5) defines the *inductance* L [Henries] of any inductor. Therefore L_1 for a single-turn current loop having length $W \gg d$ and area $A = Dd$ is:

$$L_1 = \frac{\mu D d}{W} = \frac{\mu A}{W} \text{ [H]} \quad (\text{single-turn wide inductor}) \quad (3.2.6)$$

To simplify these equations we define *magnetic flux* ψ_m as⁸:

$$\psi_m = \iint_A \mu \bar{H} \cdot d\bar{a} \text{ [Webers = Vs]} \quad (3.2.7)$$

Then Equations (3.2.4) and (3.2.7) become:

$$v(t) = d\psi_m(t)/dt \quad (3.2.8)$$

$$\psi_m(t) = L i(t) \quad (\text{single-turn inductor}) \quad (3.2.9)$$

⁸ The symbol ψ_m for magnetic flux [Webers] should not be confused with Ψ for magnetic potential [Amperes].

Since we assumed fringing fields could be neglected because $W \gg d$, large single-turn inductors require very large structures. The standard approach to increasing inductance L in a limited volume is instead to use multi-turn coils as illustrated in Figure 3.2.3.

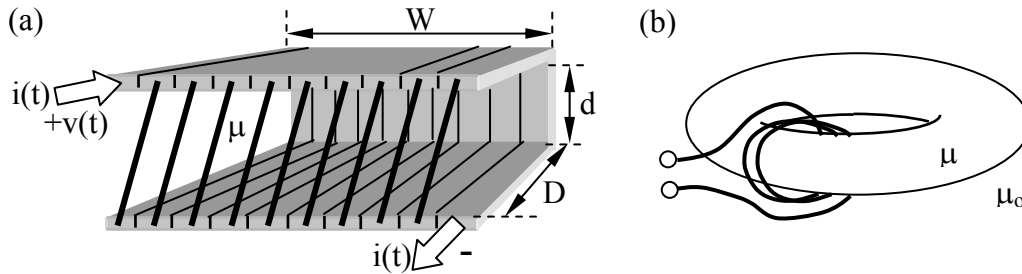


Figure 3.2.3 N-turn inductor: (a) solenoid, (b) toroid.

The N-turn coil of Figure 3.2.3 duplicates the current flow geometry illustrated in Figures 3.2.1 and 3.2.2, but with N times the intensity ($A \text{ m}^{-1}$) for the same terminal current $i(t)$, and therefore the magnetic field H_0 and flux ψ_m are also N times stronger than before. At the same time the voltage induced in each turn is proportional to the flux ψ_m through it, which is now N times greater than for a single-turn coil ($\psi_m = Ni\mu A/W$), and the total voltage across the inductor is the sum of the voltages across the N turns. Therefore, provided that $W \gg d$, the total voltage across an N-turn inductor is N^2 times its one-turn value, and the inductance L_N of an N-turn coil is also N^2 greater than L_1 for a one-turn coil:

$$v(t) = L_N \frac{di(t)}{dt} = N^2 L_1 \frac{di(t)}{dt} \quad (3.2.10)$$

$$L_N = N^2 \frac{\mu A}{W} \quad [\quad] \quad (\text{N-turn solenoidal inductor}) \quad (3.2.11)$$

where A is the coil area and W is its length; $W \gg \sqrt{A} > d$.

Equation (3.2.11) also applies to cylindrical coils having $W \gg d$, which is the most common form of inductor. To achieve large values of N the turns of wire can be wound on top of each other with little adverse effect; (3.2.11) still applies.

These expressions can also be simplified by defining *magnetic flux linkage* Λ as the magnetic flux ψ_m (3.2.7) linked by N turns of the current i , where:

$$\Lambda = N\psi_m = N(Ni\mu A/W) = (N^2\mu A/W)i = Li \quad (\text{flux linkage}) \quad (3.2.12)$$

This equation $\Lambda = Li$ is dual to the expression $Q = Cv$ for capacitors. We can use (3.2.5) and (3.2.12) to express the voltage v across N turns of a coil as:

$$v = L di/dt = d\Lambda/dt \quad (\text{any coil linking magnetic flux } \Lambda) \quad (3.2.13)$$

The net inductance L of two inductors L_1 and L_2 in series or parallel is related to L_1 and L_2 in the same way two connected resistors are related:

$$L = L_1 + L_2 \quad (\text{series combination}) \quad (3.2.14)$$

$$L^{-1} = L_1^{-1} + L_2^{-1} \quad (\text{parallel combination}) \quad (3.2.15)$$

For example, two inductors in series convey the same current i but the total voltage across the pair is the sum of the voltages across each – so the inductances add.

Example 3.2A

Design a 100-Henry air-wound inductor.

Solution: Equation (3.2.11) says $L = N^2\mu A/W$, so N and the form factor A/W must be chosen. Since $A = \pi r^2$ is the area of a cylindrical inductor of radius r , then $W = 4r$ implies $L = N^2\mu\pi r/4$. Although tiny inductors (small r) can be achieved with a large number of turns N , N is limited by the ratio of the cross-sectional areas of the coil rW and of the wire πr_w^2 , and is $N \cong r^2/r_w^2$. N is further limited if we want the resistive impedance $R \ll j\omega L$. If ω_{\min} is the lowest frequency of interest, then we want $R \cong \omega_{\min}L/100 = d/(\sigma\pi r_w^2)$ [see (3.1.5)], where the wire length $d \cong 2\pi rN$. These constraints eventually yield the desired values for r and N that yield the smallest inductor. Example 3.2B carries these issues further.

3.2.2 Toroidal inductors

The prior discussion assumed μ filled all space. If μ is restricted to the interior of a solenoid, L is diminished significantly, but coils wound on a high- μ *toroid*, a donut-shaped structure as illustrated in Figure 3.2.3(b), yield the full benefit of high values for μ . Typical values of μ are ~ 5000 to $180,000$ for iron, and up to $\sim 10^6$ for special materials.

Coils wound on high-permeability toroids exhibit significantly less flux leakage than solenoids. Consider the boundary between air and a high-permeability material ($\mu/\mu_0 \gg 1$), as illustrated in Figure 3.2.4.

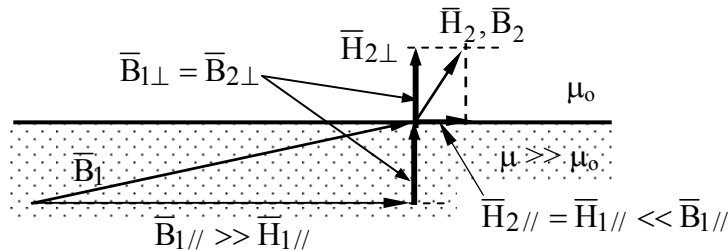


Figure 3.2.4 Magnetic fields at high-permeability boundaries.

The degree to which \bar{B} is parallel or perpendicular to the illustrated boundary has been diminished substantially for the purpose of clarity. The boundary conditions are that both \bar{B}_\perp and \bar{H}_\parallel are continuous across any interface (2.6.5, 2.6.11). Since $\bar{B} = \mu\bar{H}$ in the permeable core and $\bar{B} = \mu_0\bar{H}$ in air, and since \bar{H}_\parallel is continuous across the boundary, therefore \bar{B}_\parallel changes across the boundary by the large factor μ/μ_0 . In contrast, \bar{B}_\perp is the same on both sides. Therefore, as suggested in Figure 3.2.4, \bar{B}_2 in air is nearly perpendicular to the boundary because \bar{H}_\parallel , and therefore $\bar{B}_{2\parallel}$, is so very small; note that the figure has been scaled so that the arrows representing \bar{H}_2 and \bar{B}_2 have the same length when $\mu = \mu_0$.

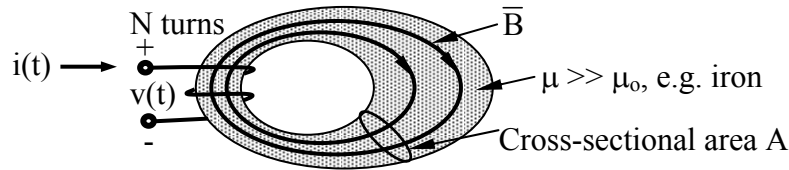


Figure 3.2.5 Toroidal inductor.

In contrast, \bar{B}_\parallel is nearly parallel to the boundary and is therefore largely trapped there, even if that boundary curves, as shown for a toroid in Figure 3.2.5. The reason magnetic flux is largely trapped within high- μ materials is also closely related to the reason current is trapped within high- σ wires, as described in Section 4.3.

The inductance of a *toroidal inductor* is simply related to the linked magnetic flux Λ by (3.2.12) and (3.2.7):

$$L = \frac{\Lambda}{i} = \frac{\mu N \iint_A \bar{H} \cdot d\bar{a}}{i} \quad (\text{toroidal inductor}) \quad (3.2.16)$$

where A is any cross-sectional area of the toroid.

Computing \bar{H} is easier if the toroid is circular and has a constant cross-section A which is small compared to the major radius R so that $R \gg \sqrt{A}$. From Ampere's law we learn that the integral of \bar{H} around the $2\pi R$ circumference of this toroid is:

$$\oint_C \bar{H} \cdot d\bar{s} \cong 2\pi R H \cong Ni \quad (3.2.17)$$

where the only linked current is $i(t)$ flowing through the N turns of wire threading the toroid. Equation (3.2.17) yields $H \cong Ni/2\pi R$ and (3.2.16) relates H to L . Therefore the inductance L of such a toroid found from (3.2.16) and (3.2.17) is:

$$L \cong \frac{\mu N A}{i} \frac{Ni}{2\pi R} = \frac{\mu N^2 A}{2\pi R} \quad [\text{Henries}] \quad (\text{toroidal inductor}) \quad (3.2.18)$$

The inductance is proportional to μ , N^2 , and cross-sectional area A , but declines as the toroid major radius R increases. The most compact large- L toroids are therefore fat (large A) with almost no hole in the middle (small R); the hole size is determined by N (made as large as possible) and the wire diameter (made small). The maximum acceptable series resistance of the inductor limits N and the wire diameter; for a given wire mass [kg] this resistance is proportional to N^2 .

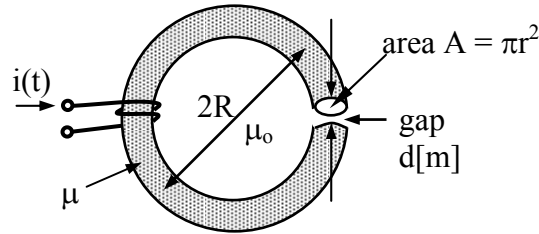


Figure 3.2.6 Toroidal inductor with a small gap.

The inductance of a high-permeability toroid is strongly reduced if even a small gap of width d exists in the magnetic path, as shown in Figure 3.2.6. The inductance L of a toroid with a gap of width d can be found using (3.2.16), but first we must find the magnitude of H_μ within the toroid. Again we can use the integral form of Ampere's law for a closed contour along the axis of the toroid, encircling the hole.

$$\oint_C \bar{H} \cdot d\bar{s} \cong (2\pi R - d)H_\mu + H_g d \cong Ni \quad (3.2.19)$$

where H_g is the magnitude of H within the gap. Since \bar{B}_\perp is continuous across the gap faces, $\mu_0 H_g = \mu H_\mu$ and these two equations can be solved for the two unknowns, H_g and H_μ . The second term $H_g d$ can be neglected if the gap width $d \ll 2\pi R \mu_0 / \mu$. In this limiting case we have the same inductance as before, (3.2.18). However, if $A^{0.5} > d \gg 2\pi R \mu_0 / \mu$, then $H_g \cong Ni/d$ and:

$$L = \Lambda/i \cong N\psi_m/i \cong N\mu_0 H_g A/i \cong N^2 \mu_0 A/d \text{ [H]} \quad (\text{toroid with a gap}) \quad (3.2.20)$$

Relative to (3.2.18) the inductance has been reduced by a factor of μ_0/μ and increased by a much smaller factor of $2\pi R/d$, a significant net reduction even though the gap is small.

Equation (3.2.20) suggests how small air gaps in magnetic motors limit motor inductance and sometimes motor torque, as discussed further in Section 6.3. Gaps can be useful too. For example, if μ is non-linear [$\mu = f(H)$], then $L \neq f(H)$ if the gap and μ_0 dominate L . Also, inductance dominated by gaps can store more energy when H exceeds saturation (i.e., $B^2/2\mu_0 \gg B_{SAT}^2/2\mu$).

3.2.3 Energy storage in inductors

The energy stored in an inductor resides in its magnetic field, which has an instantaneous energy density of:

$$W_m(t) = \mu |\bar{H}|^2 / 2 \quad [\text{J m}^{-3}] \quad (3.2.21)$$

Since the magnetic field is uniform within the volume Ad of the rectangular inductor of Figure 3.2.1, the total instantaneous magnetic energy stored there is:

$$w_m \cong \mu AW |\bar{H}|^2 / 2 \cong \mu AW (i/W)^2 / 2 \cong Li^2 / 2 \quad [\text{J}] \quad (3.2.22)$$

That (3.2.22) is valid and exact for any inductance L can be shown using Poynting's theorem, which relates power $P = vi$ at the device terminals to changes in energy storage:

$$w_m = \int_{-\infty}^t v(t) i(t) dt = \int_{-\infty}^t L (di/dt) i dt = \int_0^i Li di = Li^2 / 2 [\text{J}] \quad (3.2.23)$$

Earlier we neglected fringing fields, but they store magnetic energy too. We can compute them accurately using the Biot-Savart law (10.2.21), which is derived later and expresses \bar{H} directly in terms of the currents flowing in the inductor:

$$\bar{H}(\bar{r}) = \iiint_{V'} dv' [\bar{J}(\bar{r}') \times (\bar{r} - \bar{r}')] / [4\pi |\bar{r} - \bar{r}'|^3] \quad (3.2.24)$$

The magnetic field produced by current $\bar{J}(\bar{r}')$ diminishes with distance squared, and therefore the magnitude of the uniform field \bar{H} within the inductor is dominated by currents within a distance of $\sim d$ of the inductor ends, where d is the nominal diameter or thickness of the inductor [see Figure 3.2.3(a) and assume $d \cong D \ll W$]. Therefore $|\bar{H}|$ at the center of the end-face of a semi-infinite cylindrical inductor has precisely half the strength it has near the middle of the same inductor because the Biot-Savart contributions to \bar{H} at the end-face arise only from one side of the end-face, not from both sides.

The energy density within a solenoidal inductor therefore diminishes within a distance of $\sim d$ from each end, but this is partially compensated in (3.2.23) by the neglected magnetic energy outside the inductor, which also decays within a distance $\sim d$. For these reasons fringing fields are usually neglected in inductance computations when $d \ll W$. Because magnetic flux is non-divergent, the reduced field intensity near the ends of solenoids implies that some magnetic field lines escape the coil there; they are fully trapped within the rest of the coil.

The energy stored in a thin toroidal inductor can be found using (3.2.21):

$$w_m \cong \left(\mu |\bar{H}|^2 / 2 \right) A 2\pi R \quad (3.2.25)$$

The energy stored in a toroidal inductor with a non-negligible gap of width d can be easily found knowing that the energy storage in the gap dominates that in the high-permeability toroid, so that:

$$w_m \cong (\mu_o H_g^2 / 2) Ad \cong \mu_o (Ni/d)^2 Ad/2 \cong Li^2/2 \quad (3.2.26)$$

Example 3.2B

Design a practical 100-Henry inductor wound on a toroid having $\mu = 10^4 \mu_o$; it is to be used for $\omega \cong 400$ [r s⁻¹] (~60 Hz). How many Joules can it store if the current is one Ampere? If the residual flux density B_r of the toroid is 0.2 Tesla, how does this affect design?

Solution: We have at least three unknowns, i.e., size, number of turns N , and wire radius r_w , and therefore need at least three equations. Equation (3.2.18) says $L \cong \mu N^2 A / 2\pi R_m$ where $A = \pi r^2$. A fat toroid might have major radius $R_m \cong 3r$, corresponding to a central hole of radius $2r$ surrounded by an iron torus $2r$ thick, yielding an outer diameter of $4r$. Our first equation follows: $L = 100 \cong \mu N^2 r / 6$. Next, the number N of turns is limited by the ratio of the cross-sectional area of the hole in the torus ($\pi 4r^2$) and the cross-sectional area of the wire πr_w^2 ; our second equation is $N \cong 4r^2 / r_w^2$. Although tiny inductors (small r) can be achieved with large N , N is limited if we want the resistive impedance $R \ll \omega L$. If ω_{\min} is the lowest frequency of interest, then we obtain our third equation, $R \cong \omega_{\min} L / 100 = 400 = d / (\sigma \pi r_w^2)$ [see (3.1.5)], where the wire length $d \cong 4\pi r N$. Eliminating r_w^2 from the second and third equation yields $N^2 \cong 400 \sigma r$, and eliminating N^2 from the first equation yields $r = (600 / 400 \sigma \mu)^{0.5} \cong 1.5$ mm, where for typical wires $\sigma \cong 5 \times 10^7$; the maximum diameter of this toroid is $8r \cong 1.2$ cm. Since $N^2 \cong 400 \sigma r$, therefore $N \cong 5600$, and $r_w \cong 2r / \sqrt{N} \cong 40$ microns.

We might suppose the stored energy $w_m = Li^2/2 = 100 \times 1^2 / 2 = 50$ joules. However, if 1 ampere flows through 5600 turns, and if $H = 5600 / 2\pi 3r = 5600 / 0.031 = 1.8 \times 10^5$ [A m⁻¹], then $B = \mu H \cong 2300$ Tesla, well above the limit of $B_r = 0.2$ Tesla where saturation was said to occur. Since the incremental μ_o applies at high currents, this device is quite non-linear and the computed stored energy of 50J should be reduced by a factor of $\sim \mu_o / \mu$ to yield ~ 5 mJ. If linearity and low loss ($R \ll \omega L$) are desired, either this toroid must be made much larger so that the upper limit on μH inside the toroid is not exceeded, or the maximum current must be reduced to the ~ 100 μA level. Moreover, a sinusoidal current of 1 ampere through this small 400-ohm resistance would dissipate 200 W, enough to damage it. Note that if ω_{\min} is increased by a factor of F , then r decreases by $F^{0.5}$.

3.2.4 Transformers

Transformers are passive devices used to raise or lower the voltages of alternating currents or transients. The voltage v across two terminals of any coil can be found using Faraday's law (2.4.14):

$$\oint_C \bar{E} \cdot d\bar{s} = -\frac{d}{dt} \iint_A \mu_0 \bar{H} \cdot d\bar{a} \quad (3.2.27)$$

which leads to the voltage across any N turns of a coil, as given by (3.2.13):

$$v = d\Lambda/dt \quad (3.2.28)$$

where the flux linkage $\Lambda = N\psi_m$ and the magnetic flux ψ_m within the cross-sectional area A of the coil is defined by (3.2.7):

$$\Psi_m = \iint_A \mu \bar{H} \cdot d\bar{a} \quad [\text{Webers} = \text{Vs}] \quad (3.2.29)$$

Consider the ideal toroidal transformer of Figure 3.2.7.

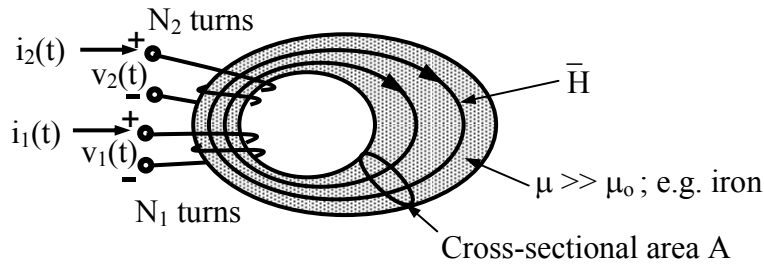


Figure 3.2.7 Toroidal transformer.

Its high permeability traps the magnetic flux within it so that ψ_m is constant around the toroid, even though A varies. From (3.2.28) we see that the voltage v_k across coil k is therefore:

$$v_k = d\Lambda_k/dt = N_k d\Psi_m/dt \quad (3.2.30)$$

The ratio between the voltages across two coils $k = 1,2$ is therefore:

$$v_2/v_1 = N_2/N_1 \quad (3.2.31)$$

where N_2/N_1 is the transformer turns ratio.

If current i_2 flows in the output coil, then there will be an added contribution to v_1 and v_2 due to the contributions of i_2 to the original ψ_m from the input coil alone. Note that current flowing into the “+” terminal of both coils in the figure contribute to \bar{H} in the illustrated direction; this

distinguishes the positive terminal from the negative terminal of each coil. If the flux coupling between the two coils is imperfect, then the output voltage is correspondingly reduced. Any resistance in the wires can increment these voltages in proportion to the currents.

Figure 3.2.8 suggests traditional symbols used to represent ideal transformers and some common configurations used in practice. The polarity dot at the end of each coil indicates which terminals would register the same voltage for a given change in the linked magnetic flux. In the absence of dots, the polarity indicated in (a) is understood. Note that many transformers consist of a single coil with multiple taps. Sometimes one of the taps is a commutator that can slide across the coil windings to provide a continuously variable transformer turns ratio. As illustrated, the presence of an iron core is indicated by parallel lines and an auto-transformer consists of only one tapped coil.

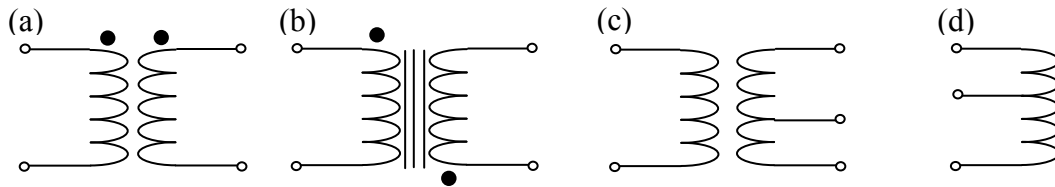


Figure 3.2.8 Transformer configurations:
 (a) air-core, (b) iron-core, (c) tapped, and (d) auto-transformer.

The terminal voltages of linear transformers for which $\mu \neq f(H)$ are linearly related to the various currents flowing through the windings. Consider a simple toroid for which H , B , and the cross-sectional area A are the same everywhere around the average circumference πD . In this case the voltage \underline{V}_1 across the N_1 turns of coil (1) is:

$$\underline{V}_1 = j\omega N_1 \quad (3.2.32)$$

$$\underline{\Psi} = \mu \underline{H} A \quad (3.2.33)$$

$$\underline{H} = (N_1 \underline{I}_1 + N_2 \underline{I}_2) / \pi D \quad (3.2.34)$$

Therefore:

$$\underline{V}_1 = j\omega [\mu A N_1 (N_1 \underline{I}_1 + N_2 \underline{I}_2) / \pi D] = j\omega (L_{11} \underline{I}_1 + L_{12} \underline{I}_2) \quad (3.2.35)$$

where the *self-inductance* L_{11} and *mutual inductance* L_{12} [Henries] are:

$$L_{11} = \mu A N_1^2 / \pi D \quad L_{12} = \mu A N_1 N_2 / \pi D \quad (3.2.36)$$

Equation (3.2.35) can be generalized for a two-coil transformer:

$$\begin{bmatrix} \underline{V}_1 \\ \underline{V}_2 \end{bmatrix} = \begin{bmatrix} L_{11} & L_{12} \\ L_{21} & L_{22} \end{bmatrix} \begin{bmatrix} \underline{I}_1 \\ \underline{I}_2 \end{bmatrix} \quad (3.2.37)$$

Consider the simple toroidal step-up transformer illustrated in Figure 3.2.9 in which the voltage source drives the load resistor R through the transformer, which has N_1 and N_2 turns on its input and output, respectively. The toroid has major diameter D and cross-sectional area A .

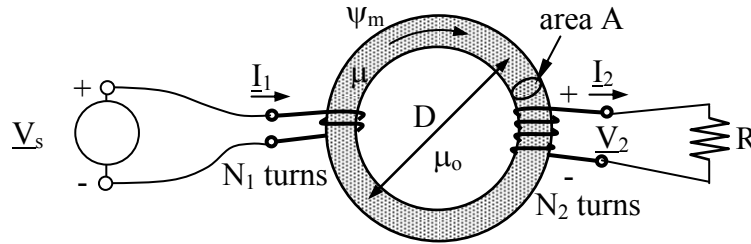


Figure 3.2.9 Toroidal step-up transformer loaded with resistor R .

Combining (3.2.33) and (3.2.34), and noting that the sign of I_2 has been reversed in the figure, we obtain the expression for total flux:

$$\underline{\Psi} = \mu A (N_1 \underline{I}_1 + N_2 \underline{I}_2) / \pi D \quad (3.2.38)$$

We can find the admittance seen by the voltage source by solving (3.2.38) for \underline{I}_1 and dividing by \underline{V}_s :

$$\underline{I}_1 = (\pi D \underline{\Psi} / \mu A N_1) + \underline{I}_2 N_2 / N_1 \quad (3.2.39)$$

$$\underline{V}_s = j\omega N_1 \underline{\Psi} = \underline{V}_2 N_1 / N_2 = \underline{I}_2 R N_1 / N_2 \quad (3.2.40)$$

$$\underline{I}_1 / \underline{V}_s = (\pi D \underline{\Psi} / \mu A N_1) / j\omega N_1 \underline{\Psi} + \underline{I}_2 N_2^2 / (N_1^2 \underline{I}_2 R) \quad (3.2.41)$$

$$= -j\pi D / (\omega N_1^2 \mu A) + (N_2 / N_1)^2 / R = 1 / j\omega L_{11} + (N_2 / N_1)^2 / R \quad (3.2.42)$$

Thus the admittance seen at the input to the transformer is that of the self-inductance ($1/j\omega L_{11}$) in parallel with the admittance of the transformed resistance $[(N_2/N_1)^2/R]$. The power delivered to the load is $|\underline{V}_2|^2/2R = |\underline{V}_1|^2(N_2/N_1)^2/2R$, which is the time-average power delivered to the transformer, since $|\underline{V}_2|^2 = |\underline{V}_1|^2(N_2/N_1)^2$; see (3.2.31).

The *transformer equivalent circuit* is thus L_{11} in parallel with the input of an ideal transformer with turns ratio N_2/N_1 . Resistive losses in the input and output coils could be represented by resistors in series with the input and output lines. Usually $j\omega L_{11}$ for an iron-core transformer is so great that only the ideal transformer is important.

One significant problem with iron-core transformers is that the changing magnetic fields within them can generate considerable voltages and *eddy currents* by virtue of Ohm's Law ($\underline{J} = \sigma \underline{E}$) and Faraday's law:

$$\oint_C \bar{\mathbf{E}} \cdot d\bar{\mathbf{s}} = -j\omega\mu \int_A \bar{\mathbf{H}} \cdot d\bar{\mathbf{a}} \quad (3.2.43)$$

where the contour C circles each conducting magnetic element. A simple standard method for reducing the eddy currents $\bar{\mathbf{J}}$ and the associated dissipated power $\int_V (\sigma|\bar{\mathbf{J}}|^2/2)dv$ is to reduce the area A by laminating the core; i.e., by fabricating it with thin stacked insulated slabs of iron or steel oriented so as to interrupt the eddy currents. The eddy currents flow perpendicular to $\bar{\mathbf{H}}$, so the slab should be sliced along the direction of $\bar{\mathbf{H}}$. If N stacked slabs replace a single slab, then A, $\bar{\mathbf{E}}$, and $\bar{\mathbf{J}}$ are each reduced roughly by a factor of N, so the power dissipated, which is proportional to the square of J, is reduced by a factor of $\sim N^2$. Eddy currents and laminated cores are discussed further at the end of Section 4.3.3.

3.3 Quasistatic behavior of devices

3.3.1 Electroquasistatic behavior of devices

The voltages and currents associated with all interesting devices sometimes vary. If the wavelength $\lambda = c/f$ associated with these variations is much larger than the device size D, no significant wave behavior can occur. The device behavior can then be characterized as electroquasistatic if the device stores primarily electric energy, and magnetoquasistatic if the device stores primarily magnetic energy. *Electroquasistatics* involves the behavior of electric fields plus the first-order magnetic consequences of their variations. The electroquasistatic approximation includes the magnetic field $\bar{\mathbf{H}}$ generated by the varying dominant electric field (Ampere's law), where:

$$\nabla \times \bar{\mathbf{H}} = \sigma\bar{\mathbf{E}} + \frac{\partial\bar{\mathbf{D}}}{\partial t} \quad (3.3.1)$$

The quasistatic approximation neglects the second-order electric field contributions from the time derivative of the resulting $\bar{\mathbf{H}}$ in Faraday's law: $\nabla \times \bar{\mathbf{E}} = -\mu_0 \partial\bar{\mathbf{H}}/\partial t \cong 0$.

One simple geometry involving slowly varying electric fields is a *capacitor* charged to voltage V(t), as illustrated in Figure 3.3.1. It consists of two circular parallel conducting plates of diameter D and area A that are separated in vacuum by the distance $d \ll D$. Boundary conditions require $\bar{\mathbf{E}}$ to be perpendicular to the plates, where $E(t) = V(t)/d$, and the surface charge density is given by (2.6.15):

$$\bar{\mathbf{E}} \cdot \hat{\mathbf{n}} = \rho_s / \epsilon_0 = V/d \quad (3.3.2)$$

$$\rho_s = \epsilon_0 V/d \quad [\text{C m}^{-2}] \quad (3.3.3)$$

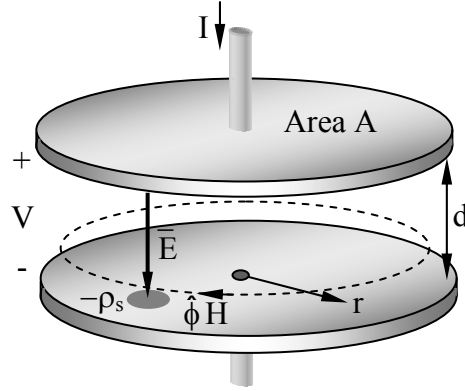


Figure 3.3.1 Quasistatic electric and magnetic fields in a circular capacitor.

Since the voltage across the plates is the same everywhere, so are \bar{E} and ρ_s , and therefore the total charge is:

$$Q(t) \cong \rho_s A \cong (\epsilon_0 A/d)V = CV(t) \quad (3.3.4)$$

where $C \cong \epsilon_0 A/d$ is the capacitance, as shown earlier (3.1.10). The same surface charge density $\rho_s(t)$ can also be found by evaluating first the magnetic field $\bar{H}(r,t)$ produced by the slowly varying (quasistatic) electric field $\bar{E}(t)$, and then the surface current $\bar{J}_s(r,t)$ associated with $\bar{H}(r,t)$; charge conservation then links $\bar{J}_s(r,t)$ to $\rho_s(t)$.

Ampere's law requires a non-zero magnetic field between the plates where $\bar{J} = 0$:

$$\oint_C \bar{H} \cdot d\bar{s} = \epsilon_0 \iint_{A'} (\partial \bar{E} / \partial t) \cdot d\bar{a} \quad (3.3.5)$$

Symmetry of geometry and excitation requires that \bar{H} between the plates be in the $\hat{\phi}$ direction and a function only of radius r , so (3.3.5) becomes:

$$2\pi r H(r) = \epsilon_0 \pi r^2 dE/dt = (\epsilon_0 \pi r^2/d) dV/dt \quad (3.3.6)$$

$$H(r) = (\epsilon_0 r/2d) dV/dt \quad (3.3.7)$$

If $V(t)$ and the magnetic field H are varying so slowly that the electric field given by Faraday's law for $H(r)$ is much less than the original electric field, then that incremental electric field can be neglected, which is the essence of the electroquasistatic approximation. If it cannot be neglected, then the resulting solution becomes more wavelike, as discussed in later sections.

The boundary condition $\hat{n} \times \bar{H} = \bar{J}_s$ (2.6.17) then yields the associated surface current $\bar{J}_s(r)$ flowing on the interior surface of the top plate:

$$\bar{J}_s(r) = \hat{r} (\epsilon_0 r/2d) dV/dt = \hat{r} J_{sr} \quad (3.3.8)$$

This in turn is related to the surface charge density ρ_s by conservation of charge (2.1.19), where the del operator is in cylindrical coordinates:

$$\nabla \cdot \bar{J}_s = -\partial\rho_s/\partial t = -r^{-1}\partial(r J_{sr})/\partial r \quad (3.3.9)$$

Substituting J_{sr} from (3.3.8) into the right-hand side of (3.3.9) yields:

$$\partial\rho_s/\partial t = (\epsilon_0/d) dV/dt \quad (3.3.10)$$

Multiplying both sides of (3.3.10) by the plate area A and integrating over time then yields $Q(t) = CV(t)$, which is the same as (3.3.4). Thus we could conclude that variations in $V(t)$ will produce magnetic fields between capacitor plates by virtue of Ampere's law and the values of either $\partial\bar{D}/\partial t$ between the capacitor plates or \bar{J}_s within the plates. These two approaches to finding \bar{H} (using $\partial\bar{D}/\partial t$ or \bar{J}_s) yield the same result because of the self-consistency of Maxwell's equations.

Because the curl of \bar{H} in Ampere's law equals the sum of current density \bar{J} and $\partial\bar{D}/\partial t$, the derivative $\partial\bar{D}/\partial t$ is often called the *displacement current* density because the units are the same, A/m^2 . For the capacitor of Figure 3.3.1 the curl of \bar{H} near the feed wires is associated only with \bar{J} (or I), whereas between the capacitor plates the curl of \bar{H} is associated only with displacement current.

Section 3.3.4 treats the electroquasistatic behavior of electric fields within conductors and relaxation phenomena.

3.3.2 Magnetoquasistatic behavior of devices

All currents produce magnetic fields that in turn generate electric fields if those magnetic fields vary. *Magnetoquasistatics* characterizes the behavior of such slowly varying fields while neglecting the second-order magnetic fields generated by $\partial\bar{D}/\partial t$ in Ampere's law, (2.1.6):

$$\nabla \times \bar{H} = \bar{J} + \partial\bar{D}/\partial t \cong \bar{J} \quad (\text{quasistatic Ampere's law}) \quad (3.3.11)$$

The associated electric field \bar{E} can then be found from Faraday's law:

$$\nabla \times \bar{E} = -\partial\bar{B}/\partial t \quad (\text{Faraday's law}) \quad (3.3.12)$$

Section 3.2.1 treated an example for which the dominant effect of the quasistatic magnetic field in a current loop is voltage induced via Faraday's law, while the example of a short wire follows; both are inductors. Section 3.3.4 treats the magnetoquasistatic example of magnetic diffusion, which is dominated by currents induced by the first-order induced voltages, and resulting modification of the original magnetic field by those induced currents. In every quasistatic problem wave effects can be neglected because the associated wavelength $\lambda \gg D$, where D is the maximum device dimension.

We can roughly estimate the inductance of a short wire segment by modeling it as a perfectly conducting cylinder of radius r_0 and length D carrying a current $i(t)$, as illustrated in Figure 3.3.2. An exact computation would normally be done using computer tools designed for such tasks because analytic solutions are practical only for extremely simple geometries. In this analysis we neglect any contributions to \bar{H} from currents in nearby conductors, which requires those nearby conductors to have much larger diameters or be far away. We also make the quasistatic assumption $\lambda \gg D$.

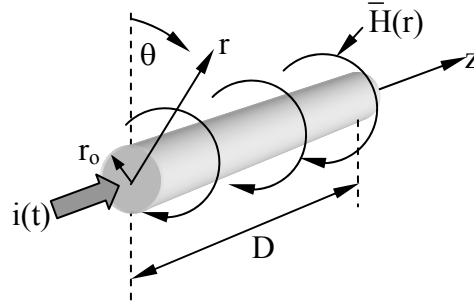


Figure 3.3.2 Inductance of an isolated wire segment.

We know from (3.2.23) that the inductance of any device can be expressed in terms of the magnetic energy stored as a function of its current i :

$$L = 2w_m/i^2 \quad [\text{H}] \quad (3.3.13)$$

Therefore to estimate L we first estimate \bar{H} and w_m . If the cylinder were infinitely long then $\bar{H} \cong \hat{\theta}H(r)$ must obey Ampere's law and exhibit the same cylindrical symmetry, as suggested in the figure. Therefore:

$$\oint_C \bar{H} \cdot d\bar{s} = 2\pi r H(r) = i(t) \quad (3.3.14)$$

and $H(r) \cong i/2\pi r$. Therefore the instantaneous magnetic energy density is:

$$\langle W_m \rangle = \frac{1}{2} \mu_0 H^2(r) = \frac{1}{2} \mu_0 (i/2\pi r)^2 \quad [\text{J/m}^3] \quad (3.3.15)$$

To find the total average stored magnetic energy we must integrate over volume. Laterally we can neglect fringing fields and simply integrate over the length D . Integration with respect to radius will produce a logarithmic answer that becomes infinite if the maximum radius is infinite. A plausible outer limit for r is $\sim D$ because the Biot-Savart law (1.4.6) says fields decrease as r^{-2} from their source if that source is local; the transition from slow cylindrical field decay as r^{-1} to decay as r^{-2} occurs at distances r comparable to the largest dimension of the source: $r \cong D$. With these approximations we find:

$$\begin{aligned}
w_m &\cong \int_0^D dz \int_{r_0}^D \langle W_m \rangle 2\pi r \, dr \cong D \int_{r_0}^D \frac{1}{2} \mu_0 \left(\frac{i}{2\pi r} \right)^2 2\pi r \, dr \\
&= (\mu_0 D i^2 / 4\pi) \ln r \Big|_{r_0}^D = (\mu_0 D i^2 / 4\pi) \ln(D/r_0) \quad [\text{J}]
\end{aligned}
\tag{3.3.16}$$

Using (3.3.13) we find the inductance L for this wire segment is:

$$L \cong (\mu_0 D / 2\pi) \ln(D/r_0) \quad [\text{Hy}] \tag{3.3.17}$$

where the units “Henries” are abbreviated here as “Hy”. Note that superposition does not apply here because we are integrating energy densities, which are squares of field strengths, and the outer limit of the integral (3.3.16) is wire length D , so longer wires have slightly more inductance than the sum of shorter elements into which they might be subdivided.

3.3.3 Equivalent circuits for simple devices

Section 3.1 showed how the parallel plate resistor of Figure 3.1.1 would exhibit resistance $R = d/\sigma A$ ohms and capacitance $C = \epsilon A/d$ farads, connected in parallel. The currents in the same device also generate magnetic fields and add inductance.

Referring to Figure 3.1.1 of the original parallel plate resistor, most of the inductance will arise from the wires, since they have a very small radius r_0 compared to that of the plates. This inductance L will be in series with the RC portions of the device because their two voltage drops add. The R and C components are in parallel because the total current through the device is the sum of the conduction current and the displacement current, and the voltages driving these two currents are the same, i.e., the voltage between the parallel plates. The corresponding first-order equivalent circuit is illustrated in Figure 3.3.3.

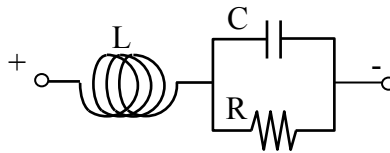


Figure 3.3.3 Equivalent RLC circuit of a parallel-plate capacitor.

Examination of Figure 3.3.3 suggests that at very low frequencies the resistance R dominates because, relative to the resistor, the inductor and capacitor become approximate short and open circuits, respectively. At the highest frequencies the inductor dominates. As f increases from zero beyond where R dominates, either the RL or the RC circuit first dominates, depending on whether C shorts the resistance R at lower frequencies than when L open-circuits R ; that is, RC dominates first when $R > \sqrt{L/C}$. At still higher frequencies the LC circuit dominates, followed by L alone. For certain combinations of R , L , and C , some transitions can merge.

Even this model for a resistor is too simple; for example, the wires also exhibit resistance and there is magnetic energy stored between the end plates because $\partial D/\partial t \neq 0$ there. Since such parasitic effects typically become important only at frequencies above the frequency range specified for the device, they are normally neglected. Even more complex behavior can result if the frequencies are so high that the device dimensions exceed $\sim \lambda/8$, as discussed later in Section 7.1. Similar considerations apply to every resistor, capacitor, inductor, or transformer manufactured. Components and circuits designed for very high frequencies minimize unwanted *parasitic capacitance* and *parasitic inductance* by their very small size and proper choice of materials and geometry. It is common for circuit designers using components or wires near their design limits to model them with simple lumped-element equivalent circuits like that of Figure 3.3.3, which include the dominant parasitic effects. The form of these circuits obviously depends on the detailed structure of the modeled device; for example, R and C might be in series.

Example 3.3A

What are the approximate values L and C for the 100- Ω resistor designed in Example 3.1A if $\epsilon = 4\epsilon_0$, and what are the three critical frequencies $(RC)^{-1}$, R/L , and $(LC)^{-0.5}$?

Solution: The solution to 3.1A said the conducting caps of the resistor have area $A = \pi r^2 = \pi(2.5 \times 10^{-4})^2$, and the length of the dielectric d is 1 mm. The permittivity $\epsilon = 4\epsilon_0$, so the capacitance (3.1.10) is $C = \epsilon A/d = 4 \times 8.85 \times 10^{-12} \times \pi(2.5 \times 10^{-4})^2/10^{-3} \cong 7 \times 10^{-15}$ farads. The inductance L of this device would probably be dominated by that of the connecting wires because their diameters would be smaller and their length longer. Assume the wire length is $D = 4d = 4 \times 10^{-3}$, and its radius r is 10^{-4} . Then (3.3.17) yields $L \cong (\mu_0 D/16\pi) \ln(D/r) = (1.26 \times 10^{-6} \times 4 \times 10^{-3}/16\pi) \ln(40) = 3.7 \times 10^{-10}$ [Hy]. The critical frequencies R/L , $(RC)^{-1}$, and $(LC)^{-0.5}$ are 2.7×10^{11} , 6.2×10^{11} , and 1.4×10^{12} [$r\ s^{-1}$], respectively, so the maximum frequency for which reasonably pure resistance is obtained is ~ 10 GHz ($\sim R/2\pi L4$).

3.4 General circuits and solution methods

3.4.1 Kirchoff's laws

Circuits are generally composed of *lumped elements* or “*branches*” connected at *nodes* to form two- or three-dimensional structures, as suggested in Figure 3.4.1. They can be characterized by the voltages v_i at each node or across each branch, or by the currents i_j flowing in each branch or in a set of current loops. To determine the behavior of such circuits we develop simultaneous linear equations that must be satisfied by the unknown voltages and currents. Kirchoff's laws generally provide these equations.

Although circuit analysis is often based in part on Kirchoff's laws, these laws are imperfect due to electromagnetic effects. For example, *Kirchoff's voltage law* (KVL) says that the voltage drops v_i associated with each lumped element around any loop must sum to zero, i.e.:

$$\sum_i v_i = 0 \quad \text{(Kirchoff's voltage law [KVL])} \quad (3.4.1)$$

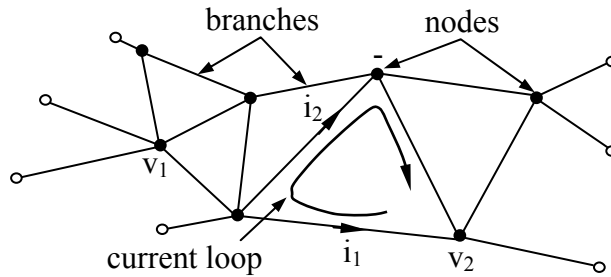


Figure 3.4.1 Circuit with branches and current loops.

which can be derived from the integral form of Faraday's law:

$$\oint_C \bar{E} \cdot d\bar{s} = -(\partial/\partial t) \iint_A \bar{B} \cdot d\bar{a} \quad (3.4.2)$$

This integral of $\bar{E} \cdot d\bar{s}$ across any branch yields the voltage across that branch. Therefore the sum of branch voltages around any closed contour is zero if the net magnetic flux through that contour is constant; this is the basic assumption of KVL.

KVL is clearly valid for any static circuit. However, any branch carrying time varying current will contribute time varying magnetic flux and therefore voltage to all adjacent loops plus others nearby. These voltage contributions are typically negligible because the currents and loop areas are small relative to the wavelengths of interest ($\lambda = c/f$) and the KVL approximation then applies. A standard approach to analyzing circuits that violate KVL is to determine the magnetic energy or inductance associated with any extraneous magnetic fields, and to model their effects in the circuit with a lumped *parasitic inductance* in each affected current loop.

The companion relation to KVL is *Kirchoff's current law* (KCL), which says that the sum of the currents i_j flowing into any node is zero:

$$\sum_j i_j = 0 \quad (\text{Kirchoff's current law}) \quad (3.4.3)$$

This follows from conservation of charge (2.4.19) when no charge storage on the nodes is allowed:

$$(\partial/\partial t) \iiint_V \rho \, dv = -\iint_A \bar{J} \cdot d\bar{a} \quad (\text{conservation of charge}) \quad (3.4.4)$$

If no charge can be stored on the volume V of a node, then $(\partial/\partial t) \iiint_V \rho \, dv = 0$, and there can be no net current into that node.

For static problems, KCL is exact. However, the physical nodes and the wires connecting those nodes to lumped elements typically exhibit varying voltages and \bar{D} , and therefore have

capacitance and the ability to store charge, violating KCL. If the frequency is sufficiently high that such *parasitic capacitance* at any node becomes important, that parasitic capacitance can be modeled as an additional lumped element attached to that node.

3.4.2 Solving circuit problems

To determine the behavior of any given linear lumped element circuit a set of simultaneous equations must be solved, where the number of equations must equal or exceed the number of unknowns. The unknowns are generally the voltages and currents on each branch; if there are b branches there are $2b$ unknowns.

Figure 3.4.2(a) illustrates a simple circuit with $b = 12$ branches, $p = 6$ loops, and $n = 7$ nodes. A set of *loop currents* uniquely characterizes all currents if each loop circles only one “hole” in the topology and if no additional loops are added once every branch in the circuit is incorporated in at least one loop. Although other definitions for the loop currents can adequately characterize all *branch currents*, they are not explored here. Figure 3.4.2(b) illustrates a bridge circuit with $b = 6$, $p = 3$, and $n = 4$.

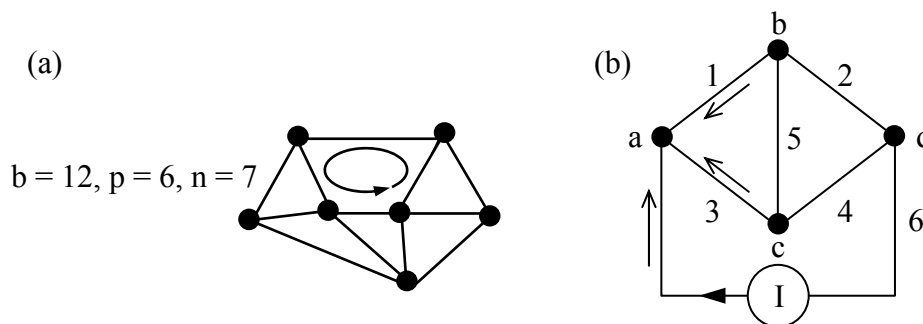


Figure 3.4.2 12-branch circuit and bridge circuit.

The simplest possible circuit has one node and one branch, as illustrated in Figure 3.4.3(a).

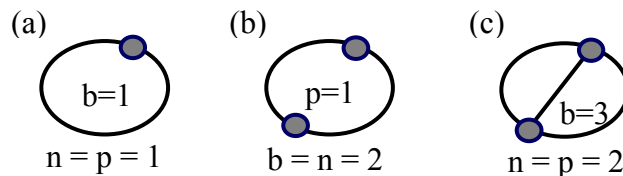


Figure 3.4.3 Simple circuit topologies; n , p , and b are the numbers of nodes, loops, and branches, respectively.

It is easy to see from the figure that the number b of branches in a circuit is:

$$b = n + p - 1 \tag{3.4.5}$$

As we add either nodes or branches to the illustrated circuit in any sequence and with any placement, Equation (3.4.5) is always obeyed. If we add voltage or current sources to the circuit, they too become branches.

The voltage and current for each branch are initially unknown and therefore any circuit has $2b$ unknowns. The number of equations is also $b + (n - 1) + p = 2b$, where the first b in this expression corresponds to the equations relating voltage to current in each branch, $n-1$ is the number of independent KCL equations, and p is the number of loops and KVL equations; (3.4.5) says $(n - 1) + p = b$. Therefore, since the numbers of unknowns and linear equations match, we may solve them. The equations are linear because Maxwell's equations are linear for RLC circuits.

Often circuits are so complex that it is convenient for purposes of analysis to replace large sections of them with either a two-terminal *Thevenin equivalent circuit* or *Norton equivalent circuit*. This can be done only when that circuit is incrementally linear with respect to voltages imposed at its terminals. Thevenin equivalent circuits consist of a voltage source $V_{Th}(t)$ in series with a passive linear circuit characterized by its frequency-dependent impedance $\underline{Z}(\omega) = R + jX$, while Norton equivalent circuits consist of a current source $I_{No}(t)$ in parallel with an impedance $\underline{Z}(\omega)$.

An important example of the utility of equivalent circuits is the problem of designing a *matched load* $\underline{Z}_L(\omega) = R_L(\omega) + jX_L(\omega)$ that accepts the maximum amount of power available from a linear source circuit, and reflects none. The solution is simply to design the load so its impedance $\underline{Z}_L(\omega)$ is the complex conjugate of the source impedance: $\underline{Z}_L(\omega) = \underline{Z}^*(\omega)$. For both Thevenin and Norton equivalent sources the reactance of the matched load cancels that of the source [$X_L(\omega) = -X(\omega)$] and the two resistive parts are set equal, $R = R_L$.

One proof that a matched load maximizes power transfer consists of computing the time-average power P_d dissipated in the load as a function of its impedance, equating to zero its derivative $dP_d/d\omega$, and solving the resulting complex equation for R_L and X_L . We exclude the possibility of negative resistances here unless those of the load and source have the same sign; otherwise the transferred power can be infinite if $R_L = -R$.

Example 3.4A

The *bridge circuit* of Figure 3.4.2(b) has five branches connecting four nodes in every possible way except one. Assume both parallel branches have 0.1-ohm and 0.2-ohm resistors in series, but in reverse order so that $R_1 = R_4 = 0.1$, and $R_2 = R_3 = 0.2$. What is the resistance R of the bridge circuit between nodes a and d if $R_5 = 0$? What is R if $R_5 = \infty$? What is R if R_5 is 0.5 ohms?

Solution: When $R_5 = 0$ then the node voltages $v_b = v_c$, so R_1 and R_3 are connected in parallel and have the equivalent resistance $R_{13//}$. Kirchoff's current law "KCL" (3.4.3) says the current flowing into node "a" is $I = (v_a - v_b)(R_1^{-1} + R_3^{-1})$. If $V_{ab} \equiv (v_a - v_b)$, then $V_{ab} = IR_{13//}$ and $R_{13//} = (R_1^{-1} + R_3^{-1})^{-1} = (10+5)^{-1} = 0.067\Omega = R_{24//}$. These two circuits are in series so their resistances add: $R = R_{13//} + R_{24//} \cong 0.133$ ohms. When $R_5 = \infty$, R_1

and R_2 are in series with a total resistance R_{12s} of $0.1 + 0.2 = 0.3\Omega = R_{34s}$. These two resistances, R_{12s} and R_{34s} are in parallel, so $R = (R_{12s}^{-1} + R_{34s}^{-1})^{-1} = 0.15\Omega$. When R_5 is finite, then simultaneous equations must be solved. For example, the currents flowing into each of nodes a, b, and c sum to zero, yielding three simultaneous equations that can be solved for the vector $\bar{V} = [v_a, v_b, v_c]$; we define $v_d = 0$. Thus $(v_a - v_b)/R_1 + (v_a - v_c)/R_3 = I = v_a(R_1^{-1} + R_3^{-1}) - v_bR_1^{-1} - v_cR_3^{-1} = 15v_a - 10v_b - 5v_c$. KCL for nodes b and c similarly yield: $-10v_a + 17v_b - 2v_c = 0$, and $-5v_a - 2v_b + 17v_c = 0$. If we define the current vector $\bar{I} = [I, 0, 0]$, then these three equations can be written as a matrix equation:

$$\bar{G}\bar{v} = \bar{I}, \text{ where } \bar{G} = \begin{bmatrix} 15 & -10 & -5 \\ -10 & 17 & -2 \\ -5 & -2 & 17 \end{bmatrix}.$$

Since the desired circuit resistance between nodes a and d is $R = v_a/I$, we need only solve for v_a in terms of I , which follows from $\bar{v} = \bar{G}^{-1}\bar{I}$, provided the conductance matrix \bar{G} is not singular (here it is not). Thus $R = 0.146\Omega$, which is intermediate between the first two solutions, as it should be.

3.5 Two-element circuits and RLC resonators

3.5.1 Two-element circuits and uncoupled RLC resonators

RLC resonators typically consist of a resistor R , inductor L , and capacitor C connected in series or parallel, as illustrated in Figure 3.5.1. RLC resonators are of interest because they behave much like other electromagnetic systems that store both electric and magnetic energy, which slowly dissipates due to resistive losses. First we shall find and solve the differential equations that characterize RLC resonators and their simpler sub-systems: RC, RL, and LC circuits. This will lead to definitions of resonant frequency ω_0 and Q , which will then be related in Section 3.5.2 to the frequency response of RLC resonators that are coupled to circuits.

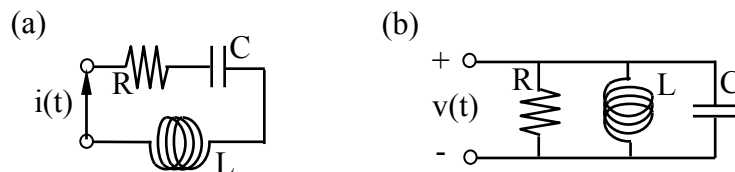


Figure 3.5.1 Series and parallel RLC resonators.

The differential equations that govern the voltages across R 's, L 's, and C 's are, respectively:

$$v_R = iR \tag{3.5.1}$$

$$v_L = L di/dt \quad (3.5.2)$$

$$v_C = (1/C) \int i dt \quad (3.5.3)$$

Kirchoff's voltage law applied to the series RLC circuit of Figure 3.5.1(a) says that the sum of the voltages (3.5.1), (3.5.2), and (3.5.3) is zero:

$$d^2i/dt^2 + (R/L) di/dt + (1/LC)i = 0 \quad (3.5.4)$$

where we have divided by L and differentiated to simplify the equation. Before solving it, it is useful to solve simpler versions for RC, RL, and LC circuits, where we ignore one of the three elements.

In the RC limit where $L = 0$ we add (3.5.1) and (3.5.3) to yield the differential equation:

$$di/dt + (1/RC)i = 0 \quad (3.5.5)$$

This says that $i(t)$ can be any function with the property that the first derivative is the same as the original signal, times a constant. This property is restricted to exponentials and their sums, such as sines and cosines. Let's represent $i(t)$ by $I_0 e^{st}$, where:

$$i(t) = \text{Re} \left\{ I_0 e^{st} \right\} \quad (3.5.6)$$

where the *complex frequency* s is:

$$s \equiv \alpha + j\omega \quad (3.5.7)$$

We can substitute (3.5.6) into (3.5.5) to yield:

$$\text{Re} \left\{ \left[s + (1/RC) \right] I_0 e^{st} \right\} = 0 \quad (3.5.8)$$

Since e^{st} is not always zero, to satisfy (3.5.8) it follows that $s = -1/RC$ and:

$$i(t) = I_0 e^{-(1/RC)t} = I_0 e^{-t/\tau} \quad (\text{RC current response}) \quad (3.5.9)$$

where τ equals RC seconds and is the *RC time constant*. I_0 is chosen to satisfy initial conditions, which were not given here.

A simple example illustrates how initial conditions can be incorporated in the solution. We simply need as many equations for $t = 0$ as there are unknown variables. In the present case we need one equation to determine I_0 . Suppose the RC circuit [of Figure 3.5.1(a) with $L = 0$] was at

rest at $t = 0$, but the capacitor was charged to V_0 volts. Then we know that the initial current I_0 at $t = 0$ must be V_0/R .

In the RL limit where $C = \infty$ we add (3.5.1) and (3.5.2) to yield $di/dt + (R/L)i = 0$, which has the same form of solution (3.5.6), so that $s = -R/L$ and:

$$i(t) = I_0 e^{-(R/L)t} = I_0 e^{-t/\tau} \quad (\text{RL current response}) \quad (3.5.10)$$

where the *RL time constant* τ is L/R seconds.

In the LC limit where $R = 0$ we add (3.5.2) and (3.5.3) to yield:

$$d^2i/dt^2 + (1/LC)i = 0 \quad (3.5.11)$$

Its solution also has the form (3.5.6). Because $i(t)$ is real and $e^{j\omega t}$ is complex, it is easier to assume sinusoidal solutions, where the phase ϕ and magnitude I_0 would be determined by initial conditions. This form of the solution would be:

$$i(t) = I_0 \cos(\omega_0 t + \phi) \quad (\text{LC current response}) \quad (3.5.12)$$

where $\omega_0 = 2\pi f_0$ is found by substituting (3.5.12) into (3.5.11) to yield $[\omega_0^2 - (LC)^{-1}]i(t) = 0$, so:

$$\omega_0 = \frac{1}{\sqrt{LC}} \quad [\text{radians s}^{-1}] \quad (\text{LC resonant frequency}) \quad (3.5.13)$$

We could alternatively express this solution (3.5.12) as the sum of two exponentials using the identity $\cos \omega t \equiv (e^{j\omega t} + e^{-j\omega t})/2$.

RLC circuits exhibit both oscillatory resonance and exponential decay. If we substitute the generic solution $I_0 e^{st}$ (3.5.6) into the RLC differential equation (3.5.4) for the *series RLC resonator* of Figure 3.5.1(a) we obtain:

$$(s^2 + sR/L + 1/LC)I_0 e^{st} = (s - s_1)(s - s_2)I_0 e^{st} = 0 \quad (3.5.14)$$

The RLC resonant frequencies s_1 and s_2 are solutions to (3.5.14) and can be found by solving this *quadratic equation*⁹ to yield:

$$s_i = -R/2L \pm j \left[(1/LC) - (R/2L)^2 \right]^{0.5} \quad (\text{series RLC resonant frequencies}) \quad (3.5.15)$$

When $R = 0$ this reduces to the LC resonant frequency solution (3.5.13).

⁹ A quadratic equation in x has the form $ax^2 + bx + c = 0$ and the solution $x = (-b \pm [b^2 - 4ac]^{0.5})/2a$.

The generic solution $i(t) = I_0' e^{st}$ is complex, where $I_0' \equiv I_0 e^{j\phi}$:

$$i(t) = \mathcal{R}_e \{ I_0' e^{s_1 t} \} = \mathcal{R}_e \{ I_0 e^{j\phi} e^{-(R/2L)t} e^{j\omega t} \} = I_0 e^{-(R/2L)t} \cos(\omega t + \phi) \quad (3.5.16)$$

where $\omega = [(LC)^{-1} + (R/2L)^2]^{0.5} \cong (LC)^{-0.5}$. I_0 and ϕ can be found from the initial conditions, which are the initial current through L and the initial voltage across C, corresponding to the initial energy storage terms. If we choose the time origin so that the phase $\phi = 0$, the instantaneous magnetic energy stored in the inductor (3.2.23) is:

$$w_m(t) = Li^2/2 = (LI_0^2/2) e^{-Rt/L} \cos^2 \omega t = (LI_0^2/4) e^{-Rt/L} (1 + \cos 2\omega t) \quad (3.5.17)$$

Because $w_m = 0$ twice per cycle and energy is conserved, the peak electric energy $w_e(t)$ stored in the capacitor must be intermediate between the peak magnetic energies stored in the inductor ($e^{Rt/L} LI_0^2/2$) during the preceding and following cycles. Also, since $dv_C/dt = i/C$, the cosine variations of $i(t)$ produce a sinusoidal variation in the voltage $v_C(t)$ across the capacitor. Together these two facts yield: $w_e(t) \cong (LI_0^2/2) e^{-Rt/L} \sin^2 \omega t$. If we define V_0 as the maximum initial voltage corresponding to the maximum initial current I_0 , and recall the expression (3.1.16) for $w_e(t)$, we find:

$$w_e(t) = Cv^2/2 \cong (CV_0^2/2) e^{-Rt/L} \sin^2 \omega t = (CV_0^2/4) e^{-Rt/L} (1 - \cos 2\omega t) \quad (3.5.18)$$

Comparison of (3.5.17) and (3.5.18) in combination with conservation of energy yields:

$$V_0 \cong (L/C)^{0.5} I_0 \quad (3.5.19)$$

Figure 3.5.2 illustrates how the current and energy storage decays exponentially with time while undergoing conversion between electric and magnetic energy storage at 2ω radians s^{-1} ; the time constant for current and voltage is $\tau = 2L/R$ seconds, and that for energy is L/R .

One useful way to characterize a resonance is by the dimensionless quantity Q , which is the number of radians required before the total energy w_T decays to $1/e$ of its original value, as illustrated in Figure 3.5.2(b). That is:

$$w_T = w_{T0} e^{-2\alpha t} = w_{T0} e^{-\omega t/Q} \quad [J] \quad (3.5.20)$$

The decay rate α for current and voltage is therefore simply related to Q :

$$\alpha = \omega/2Q \quad (3.5.21)$$

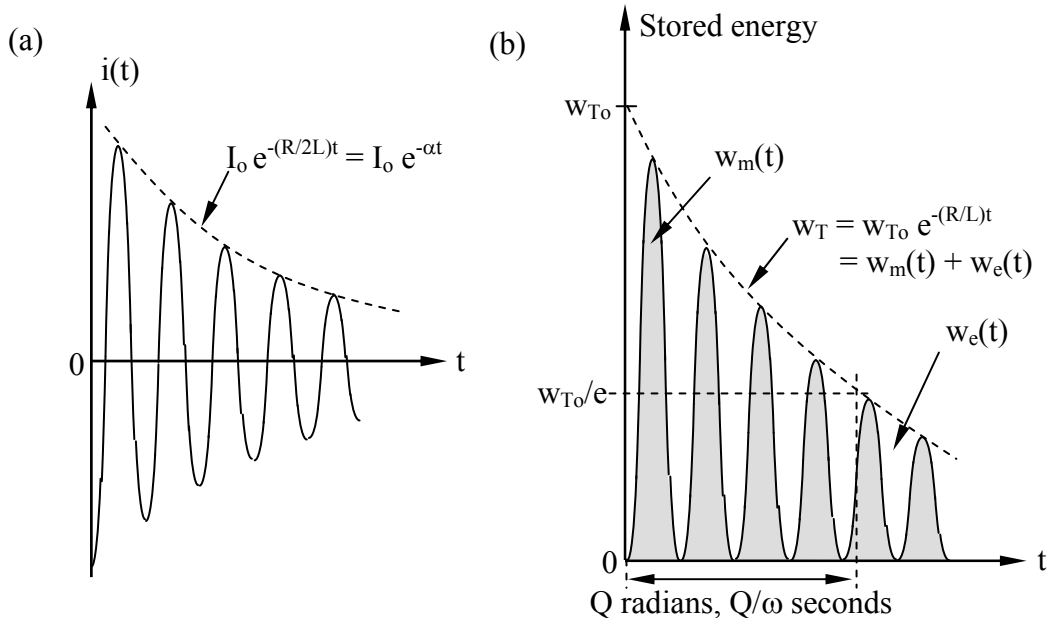


Figure 3.5.2 Time variation of current and energy storage in RLC circuits.

If we find the power dissipated P_d [W] by differentiating total energy w_T with respect to time using (3.5.20), we can then derive a common alternative definition for Q :

$$P_d = -dw_T/dt = (\omega/Q) w_T \quad (3.5.22)$$

$$Q = \omega w_T / P_d \quad (\text{one definition of } Q) \quad (3.5.23)$$

For the series RLC resonator $\alpha = R/2L$ and $\omega \cong (LC)^{-0.5}$, so (3.5.21) yields:

$$Q = \omega/2\alpha = \omega L/R \cong (L/C)^{0.5}/R \quad (Q \text{ of series RLC resonator}) \quad (3.5.24)$$

Figure 3.5.1(b) illustrates a *parallel RLC resonator*. KCL says that the sum of the currents into any node is zero, so:

$$C \, dv/dt + v/R + (1/L) \int v \, dt = 0 \quad (3.5.25)$$

$$d^2v/dt^2 + (1/RC) dv/dt + (1/LC) v = 0 \quad (3.5.26)$$

If $v = V_0 e^{st}$, then:

$$[s^2 + (1/RC)s + (1/LC)] = 0 \quad (3.5.27)$$

$$s = -(1/2RC) \pm j \left[(1/LC) - (1/2RC)^2 \right]^{0.5} \quad (\text{parallel RLC resonance}) \quad (3.5.28)$$

Analogous to (3.5.16) we find:

$$v(t) = \text{Re} \left\{ \underline{V}_0' e^{s_1 t} \right\} = V_0 e^{-(1/2RC)t} \cos(\omega t + \phi) \quad (3.5.29)$$

where $\underline{V}_0' = V_0 e^{j\phi}$. It follows that for a parallel RLC resonator:

$$\omega = \left[(LC)^{-1} - (2RC)^{-2} \right]^{0.5} \cong (LC)^{-0.5} \quad (3.5.30)$$

$$Q = \omega/2\alpha = \omega RC = R(C/L)^{0.5} \quad (\text{Q of parallel RLC resonator}) \quad (3.5.31)$$

Example 3.5A

What values of L and C would give a parallel resonator at 1 MHz a Q of 100 if $R = 10^6/2\pi$?

Solution: $LC = 1/\omega_0^2 = 1/(2\pi 10^6)^2$, and $Q = 100 = \omega RC = 2\pi 10^6(10^6/2\pi)C$ so $C = 10^{-10}$ [F] and $L = 1/\omega_0^2 c \cong 2.5 \times 10^{-4}$ [Hy].

3.5.2 Coupled RLC resonators

RLC resonators are usually coupled to an environment that can be represented by either its Thevenin or Norton equivalent circuit, as illustrated in Figure 3.5.3(a) and (b), respectively, for purely resistive circuits.

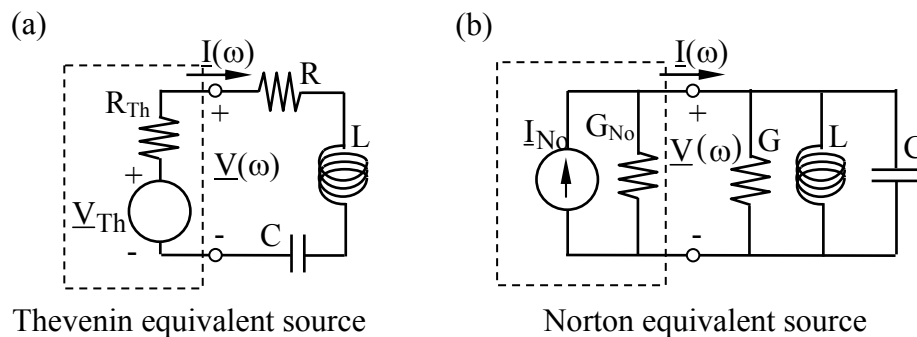


Figure 3.5.3 Series and parallel RLC resonators driven by Thevenin and Norton equivalent circuits.

A Thevenin equivalent consists of a voltage source V_{Th} in series with an impedance $\underline{Z}_{Th} = R_{Th} + jX_{Th}$, while a Norton equivalent circuit consists of a current source I_{No} in parallel with an admittance $\underline{Y}_{No} = G_{No} + jU_{No}$. The Thevenin equivalent of a resistive Norton

equivalent circuit has open-circuit voltage $V_{Th} = I_{No}/G_{No}$, and $R_{Th} = 1/G_{No}$; that is, their open-circuit voltages, short-circuit currents, and impedances are the same. No single-frequency electrical experiment performed at the terminals can distinguish ideal linear circuits from their Thevenin or Norton equivalents.

An important characteristic of a resonator is the frequency dependence of its power dissipation. If $R_{Th} = 0$, the series RLC resonator of Figure 3.5.3(a) dissipates:

$$P_d = R |I|^2 / 2 \quad [\text{W}] \quad (3.5.32)$$

$$P_d = \left[R |V_{Th}|^2 / 2 \right] / \left| R + Ls + C^{-1}s^{-1} \right|^2 = \left[R |V_{Th}|^2 / 2 \right] |s/L|^2 / \left| (s-s_1)(s-s_2) \right|^2 \quad (3.5.33)$$

where s_1 and s_2 are given by (3.5.15):

$$s_i = -R/2L \pm j \left[(1/LC) - (R/2L)^2 \right]^{0.5} = -\alpha \pm j\omega'_0 \quad (\text{series RLC resonances}) \quad (3.5.34)$$

The maximum value of P_d is achieved when $\omega \cong \omega'_0$:

$$P_{d\max} = |V_{Th}|^2 / 2R \quad (3.5.35)$$

This simple expression is expected since the reactive impedances of L and C cancel at ω_0 , leaving only R.

If $(1/LC) \gg (R/2L)$ so that $\omega_0 \cong \omega'_0$, then as $\omega - \omega_0$ increases from zero to α , $|s-s_1| = |j\omega_0 - (j\omega_0 + \alpha)|$ increases from α to $\sqrt{2}\alpha$. This departure from resonance approximately doubles the denominator of (3.5.33) and halves P_d . As ω departs still further from ω_0 and resonance, P_d eventually approaches zero because the impedances of L and C approach infinity at infinite and zero frequency, respectively. The total frequency response $P_d(f)$ of this series RLC resonator is suggested in Figure 3.5.4. The *resonator bandwidth* or *half-power bandwidth* $\Delta\omega$ is said to be the difference between the two half-power frequencies, or $\Delta\omega \cong 2\alpha = R/L$ for this series circuit. $\Delta\omega$ is simply related to ω_0 and Q for both series and parallel resonances, as follows from (3.5.21):

$$Q = \omega_0 / 2\alpha = \omega_0 / \Delta\omega \quad (\text{Q versus bandwidth}) \quad (3.5.36)$$

Parallel RLC resonators behave similarly except that:

$$s_i = -G/2L \pm j \left[(1/LC) - (G/2L)^2 \right]^{0.5} = -\alpha \pm j\omega'_0 \quad (\text{parallel RLC resonances}) \quad (3.5.37)$$

where R, L, and C in (3.5.34) have been replaced by their duals G, C, and L, respectively.

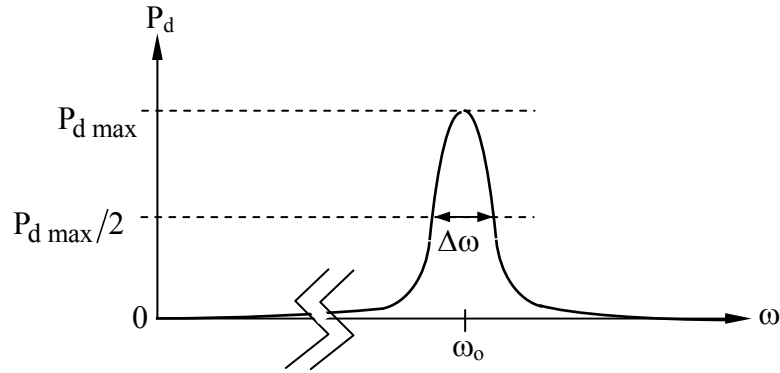


Figure 3.5.4 RLC power dissipation near resonance.

Resonators reduce to their resistors at resonance because the impedance of the LC portion approaches zero or infinity for series or parallel resonators, respectively. At resonance P_d is maximized when the source R_s and load R resistances match, as is easily shown by setting the derivative $dP_d/dR = 0$ and solving for R . In this case we say the resonator is *critically matched* to its source, for all available power is then transferred to the load at resonance.

This critically matched condition can also be related to the Q 's of a coupled resonator with zero Thevenin voltage applied from outside, where we define *internal Q* (or Q_I) as corresponding to power dissipated internally in the resonator, *external Q* (or Q_E) as corresponding to power dissipated externally in the source resistance, and *loaded Q* (or Q_L) as corresponding to the total power dissipated both internally (P_{DI}) and externally (P_{DE}). That is, following (3.5.23):

$$Q_I \equiv \omega w_T / P_{DI} \quad (\text{internal } Q) \quad (3.5.38)$$

$$Q_E \equiv \omega w_T / P_{DE} \quad (\text{external } Q) \quad (3.5.39)$$

$$Q_L \equiv \omega w_T / (P_{DI} + P_{DE}) \quad (\text{loaded } Q) \quad (3.5.40)$$

Therefore these Q 's are simply related:

$$Q_L^{-1} = Q_I^{-1} + Q_E^{-1} \quad (3.5.41)$$

It is Q_L that corresponds to $\Delta\omega$ for coupled resonators ($Q_L = \omega_0 / \Delta\omega$).

For example, by applying Equations (3.5.38–40) to a series RLC resonator, we readily obtain:

$$Q_I = \omega_0 L / R \quad (3.5.42)$$

$$Q_E = \omega_0 L / R_{Th} \quad (3.5.43)$$

$$Q_L = \omega_0 L / (R_{Th} + R) \quad (3.5.44)$$

For a parallel RLC resonator the Q's become:

$$Q_I = \omega_0 RC \quad (3.5.45)$$

$$Q_E = \omega_0 R_{Th} C \quad (3.5.46)$$

$$Q_L = \omega_0 C R_{Th} R / (R_{Th} + R) \quad (3.5.47)$$

Since the source and load resistances are matched for maximum power dissipation at resonance, it follows from Figure 3.5.3 that a *critically coupled resonator* or *matched resonator* results when $Q_I = Q_E$. These expressions for Q are in terms of energies stored and power dissipated, and can readily be applied to electromagnetic resonances of cavities or other structures, yielding their bandwidths and conditions for maximum power transfer to loads, as discussed in Section 9.4.

MIT OpenCourseWare
<http://ocw.mit.edu>

6.013 Electromagnetics and Applications
Spring 2009

For information about citing these materials or our Terms of Use, visit: <http://ocw.mit.edu/terms>.